Crystal Engineering

DOI: 10.1002/ange.201307486

Hydrolytic Conversion of a Metal–Organic Polyhedron into a Metal–Organic Framework**

*Arijit Mallick, Bikash Garai, David Díaz Díaz, and Rahul Banerjee**

Polyhedral architectures constructed with metal ions as nodes and organic ligands as linkers are generally referred to as metal–organic polyhedra (MOPs). Such architectures usually contain cavities in their cores that can be easily accessed.[1] MOPs are also known as metal–organic nanocages or metal–organic nanoballs.[2] Because of their porous structure, MOPs are capable of acting as synthetic ion channels, molecular containers for drug delivery, and molecular reaction vessels.[3,4] These 0D self-assembled cagelike structures are usually found to be readily soluble in organic solvents, which is a significant advantage, given the general drawback of the insolubility associated with extended MOF structures. Soluble MOPs can approach the target to its closest proximity and thus help the host cages to effectively encapsulate and transport guest molecules. The inclusion of different guest molecules inside a number of host MOPs is well-documented,[3] but the release of these trapped guest molecules by unfolding of the host MOP has remained unexplored. One major challenge in achieving control over the unfolding process of a MOP is to gain an understanding of the complicated chemistry behind the systematic cleavage and formation of metal–ligand bonds. This goal has motivated us to investigate the chemistry behind the unfolding of a MOP structure in the presence of reactant molecules. Although MOP–MOP interconversion is well-documented,[5] no attempts to study the unfolding of the polyhedral structure of a MOP and its subsequent conversion into a MOF have been described previously. Herein, we report an unprecedented hydrolytic conversion of a MOP, **1**, into a MOF. This transformation could be explained by a potential unfolding process of the polyhedral structure. Notably, this phenomenon resulted in the formation of a MOF, **3**, which could not be made by another method. A plausible mechanism for this transformation is also discussed, and is supported by the gradual release of encapsulated drug molecules.

Cuboctahedral crystals of **1** were synthesized by treating 5-(prop-2-ynyloxy)isophthalic acid (5PIA) with $Cu(NO_3)_2{\cdot}3H_2O$ in a 2:1 volumetric mixture of DMF and EtOH at 90 °C or in a 2:1 volumetric mixture of DMF and EtOAc at 30 °C (Scheme 1). However, a change in the solvent volumetric ratio (DMF/EtOH) from 2:1 to 1:1 caused the formation of a less crystalline and flakelike form of the MOP, **2**. This less crystalline form **2** underwent slow conversion into MOP crystals, **1**, when placed in DMF at room temperature for 2 days. Both **1** and **2** formed a blue-colored homogenous solution when heated in DMF and recrystallized into micrometer-sized crystals of **1** from a saturated solution or upon the

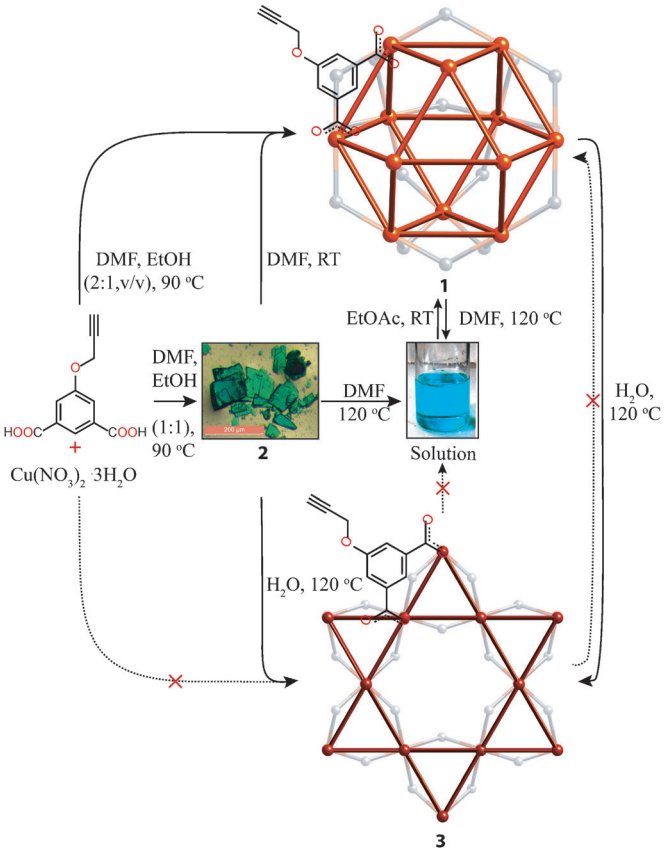

Scheme 1. Synthesis and conversion of the copper-based materials. DMF = *N*,*N*-dimethylformamide.

[*] A. Mallick,[+] B. Garai,[+] Dr. R. Banerjee
Physical/Materials Chemistry Division
CSIR-National Chemical Laboratory
Dr. Homi Bhabha Road, Pune-411008 (India)
E-mail: r.banerjee@ncl.res.in
Dr. D. D. Díaz
Institut für Organische Chemie, Universität Regensburg
Universitätsstrasse 31, 93040 Regensburg (Germany)
Dr. D. D. Díaz
IQAC-CSIC
Jordi Girona 18-26, Barcelona 08034 (Spain)
[+] These authors contributed equally.

[**] A.M. acknowledges the CSIR, New Delhi, India for a SRF, and B.G. acknowledges the UGC, New Delhi, India for a JRF. R.B. acknowledges the CSIR Five Year Plan (CSC0122 and CSC0102) for funding. Financial assistance from the BRNS (2011/37C/44/BRNS) is acknowledged.

Supporting information for this article is available on the WWW under http://dx.doi.org/10.1002/anie.201307486.

addition of EtOAc or CH_2Cl_2 at room temperature. Both types of materials underwent conversion into hexagonal crystals of **3** when heated in H_2O at 120 °C for 1 h. Notably, despite several attempts, we were unable to synthesize **3** directly by the treatment of 5PIA with different Cu^{II} salts [for example, $Cu(NO_3)_2$, $Cu(OAc)_2$].

Compound **1** crystallized in the $Im\bar{3}m$ space group in the cubic crystal system. The secondary building unit (SBU) of the structure consists of a Cu–Cu paddle-wheel center coordinated to four units of 5-(propargyloxy)isophthalate ions and two water molecules. Twelve such paddle-wheel units form a cuboctahedral structure in which the core cavity is accessible through eight triangular and six square faces (Figure 1 a). All edges of the polyhedron are decorated with

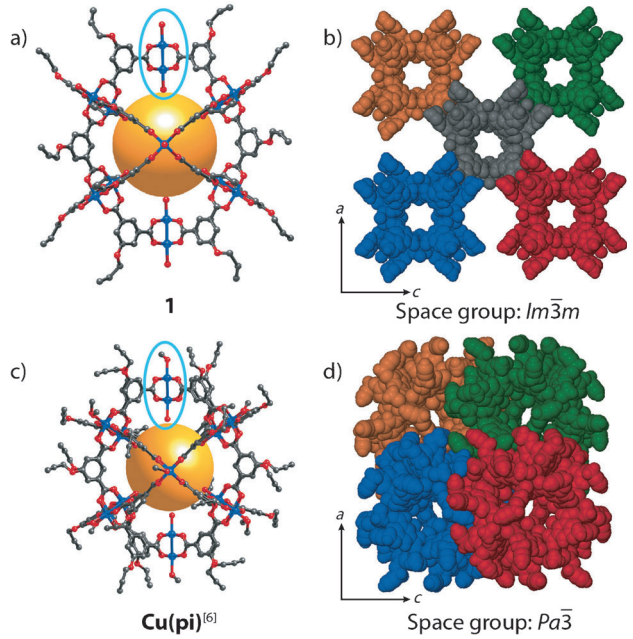

Figure 1. Structural comparison of **1** and **Cu(pi)** in terms of the coordinating solvent (highlighted by the blue ring) in their paddle-wheel SBU (a,c) and their packing in different space groups (b,d).

a propargyloxy moiety that points outwards. Each single Cu–Cu paddle-wheel SBU is connected to the adjacent SBUs through 5-(propargyloxy)isophthalate ions. All carboxylate functionalities around each of the Cu–Cu paddle-wheel SBUs of **1** point in the same direction (either upwards or downwards) and thus form a spherical assembly (Figure 1 a).

A structurally similar MOP, **Cu(pi)**, which is isomorphous to **1**, was previously synthesized by the reaction of $Cu(NO_3)_2{\cdot}3H_2O$ with 5PIA.[6] **Cu(pi)** differs from **1** in terms of the solvent molecules coordinated to the Cu–Cu paddle-wheel SBU (Figure 1 a,c) and overall crystal packing (Figure 1 b,d). Unlike **1**, **Cu(pi)** crystallizes in the $Pa\bar{3}$ space group, and thus, the packing generates a nonporous assembly (Figure 1 d). Each Cu–Cu paddle-wheel SBU of both MOPs has two axial sites available for solvent coordination. In **1**, H_2O molecules coordinate to both of these sites, whereas in the case of the **Cu(pi)** structure, Cu atoms at the inner sites of the cages are coordinated to water molecules, and Cu atoms at the outer sites are coordinated to methanol molecules. Compound **1** was found to be soluble in DMF, *N*,*N*-diethylformamide (DEF), and dimethyl sulfoxide (DMSO), whereas **Cu(pi)** remained insoluble in almost all solvents. TEM imaging indicated the presence of polyhedral MOP particles of approximately 3–4 nm in diameter in the solution of **1** in DMF (see Figure S22 in the Supporting Information). In solution in DMF, **1** and **2** showed the same UV/Vis spectrum, which was different from that of $Cu(NO_3)_2$ in solution (see Figure S17), and thus confirmed the presence of the Cu–Cu paddle-wheel structure in solution.

Compound **3** crystallized in the $P\bar{3}$ space group in the trigonal crystal system and contains a similar Cu–Cu paddle-wheel SBU to that of **1**. However, half of the carboxylate functionalities around each Cu–Cu paddle-wheel SBU are pointed in one direction, whereas the other half are pointed in the opposite direction (see Figure S6). There are two types of pores present in the extended framework of **3**. The larger pores are similar in size to the triangular face of the MOP and are hydrophilic in nature, whereas the smaller pores originate from unfolding of the MOP and are hydrophobic in nature as they contain the propargyloxy groups inside (see Figure S7).

The bulk-phase purity of all aforementioned materials was confirmed by comparison of the experimentally observed powder X-ray diffraction (PXRD) patterns with the patterns simulated from the single-crystal structures. All PXRD peaks of as-synthesized **1** and **3** matched exactly with the respective simulated patterns (see Figure S8). However, **2** showed poor crystallinity, and its PXRD pattern was different from those of **1**, **Cu(pi)**, and **3** (see Figure S9 a). MALDI-TOF analysis of **2** showed a peak at m/z 7261.02 (see Figure S13 b), which corresponds to the molecular weight of one MOP unit (M+48 H). Other studies, such as elemental analysis, FTIR spectroscopy, and solubility studies (see Figure S2), suggested that the chemical composition, metal–ligand binding, and chemical behavior of **2** were similar to those of **1**. DSC studies (see Figure S14) indicated that **2** is less crystalline in nature than **1**. The formation of nascent crystals of **1** from **2** suggested that **2** has another arrangement of MOP units with less periodicity. When **2** is dissolved, the arrangement of MOP units collapses, and discrete MOP cages/units remain in solution. Under suitable conditions, these MOP units rearrange themselves into a more stable periodic arrangement to form the crystalline form, **1** (see Figure S1).

Both **1** and **2** underwent conversion into hexagonal crystals of **3** when heated in water. Microscopic images collected at different time intervals showed that crystals of **1** in water first lose their transparency and are then converted into aggregates of hexagonal MOF crystals **3** (Figure 2 b). On the other hand, the less crystalline flakelike material **2** clearly showed conversion into hexagonal MOF crystals (Figure 2 d). Time-dependent PXRD patterns of water-treated crystals of **1** and **2** also indicated their conversion into crystals of **3** (Figure 2 a,c). As-synthesized crystals of **1** displayed coherent PXRD patterns with peak-to-peak matching with the simulated PXRD pattern. These peaks were broader at the initial stage of treatment with water, thus suggesting a decrease in crystallinity owing to the rupture of the periodic MOP crystal

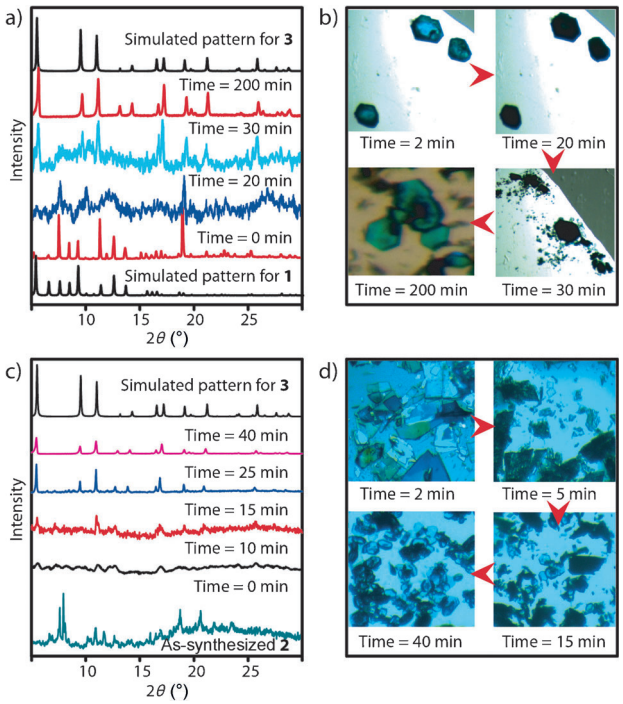

Figure 2. a) PXRD and b) microscopic monitoring of the conversion of **1** into **3** in the presence of water. c) PXRD and d) microscopic monitoring of the water-mediated conversion of **2** into **3**.

lattice. As time increased, these peaks first shifted to the positions corresponding to the pattern for **3**, then became more intense, and finally split into individual peaks that showed peak-to-peak matching with the simulated PXRD pattern of **3**. In the case of **2**, upon treatment with water, the broad peaks of the as-synthesized material first shifted to the positions corresponding to the PXRD pattern of **3**, then increased in intensity, and finally split into individual peaks that matched the simulated pattern for **3**. Similarly, when **Cu(pi)** was heated in water, it underwent polyhedral interconversion (through unfolding) and formed **3**, in the same way that **1** and **2** were converted into **3** (see Figure S10c,d).

Thermogravimetric analysis (TGA) showed that the paddle-wheel SBUs lose their coordinated water molecules at 140–185 °C in the case **1** and **2** and at 75–100 °C in the case of **3**. The MOP architecture is stable up to 250 °C, whereas the MOF structure decomposes above 280 °C. The gas-adsorption ability was moderate in the case of **1** (ca. 50 $cm^3 g^{-1}$) because of its aggregation during the activation process[7] and the resulting inaccessibility of the inner pores. However, **3** showed a BET surface area of 92 $m^2 g^{-1}$. Its water stability and the hydrophilic nature of the pores were confirmed by testing the capacity of **3** for water- and methanol-vapor adsorption. The results showed a water-vapor uptake of 176 $cm^3 g^{-1}$ and a methanol vapor adsorption of 247 $cm^3 g^{-1}$ at the standard temperature and pressure (STP; see Figure S19).

Experimental evidence pointed to a water-induced conversion of polyhedral crystals of **1** into a 2D MOF, **3**. We propose a mechanism for this phenomenon on the basis of the hypothesis that each cage has a highly hydrophobic outer surface and a less hydrophobic inner surface. This difference in hydrophobicity of the outer and inner surface of the MOP cages comes into play when these MOP crystals interact with water molecules and unfold into a MOF. The conversion of **1** or **Cu(pi)** into **3** in the presence of water is not a simple recrystallization phenomenon. In the presence of water, kinetically formed MOP units in **1** undergo conversion into thermodynamically formed MOF layers (compound **3**) by breaking, rearrangement, and the reformation of labile M–O bonds. Indeed, PXRD confirmed that this phenomenon is a solid-to-solid conversion. The UV/Vis spectrum of the filtrate isolated every 5 min during this conversion indicated that there was no trace of Cu^{II} ions in solution (see Figure S18). Owing to the porous structure of **1**, water molecules can readily diffuse into the cage and trigger the structural transition. Presumably, this unfolding occurs because of the difference in polarity between the interior and exterior surface of the polyhedron. When MOP crystals are placed in water, the outer surface, because of its higher hydrophobicity, tries to minimize its interaction with water, whereas the less hydrophobic inner core has a preference for exposure to water. This strain causes the polyhedral structure to unfold into different fragments, which undergo further rearrangement by rotation of their terminal moieties (Figure 3). These modified fragments act as building units and undergo self-assembly directed by the terminal moieties of the key building block towards the thermodynamic formation of **3**. The orientation of the terminal moieties directs the self-assembly

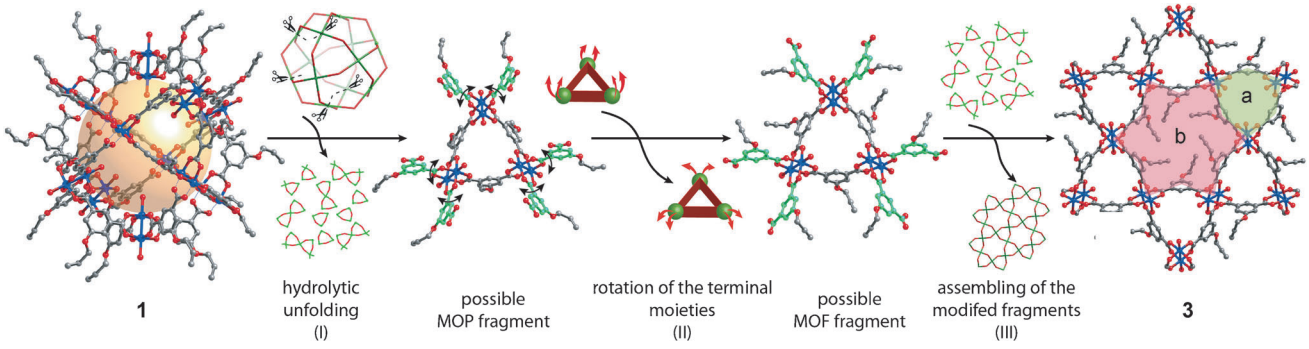

Figure 3. Proposed mechanism for the hydrolytic conversion of **1** into **3**. In step I, MOP unfolds by the attack of water at the M–O bond with the formation of different fragments. The fragments then undergo rotation of their terminal moieties to generate the "all down" arrangement of the terminal carboxylates from their "all up" position (step II), and these modified fragments undergo further self-assembly into **3** (step III).

process, as these layers stack on top of each other to form hydrophobic and hydrophilic channels (see Figure S7). This behavior can explain the initial decrease and subsequent increase in the crystallinity of the material.

Although we acknowledge that this mechanism is only a possible mechanism that is consistent with the experimental data, it is also supported by the water stability of another isostructural MOP, c-MOP-1,[8] formed from $Cu(NO_3)_2 \cdot 3H_2O$ and isophthalic acid. Owing to the absence of the propargyloxy functionality at the 5-position of the isophthalic acid moiety, the interior and the exterior surface of c-MOP-1 have a similar hydrophobic nature. Thus, the hydrophobicity gradient does not appear for c-MOP-1 when it is placed in water, thereby preventing this interconversion. In a comparative study, as-synthesized crystals of **1** and c-MOP-1 were immersed separately in water (5 mL), and the resulting samples were heated at 120 °C for 1 h. It was found that all crystals of **1** were converted into **3**, whereas c-MOP-1 remained intact (see Figure S10a,b).

This interconversion was tested as a vehicle for the release of encapsulated guest molecules. Caffeine, a widely used stimulant drug,[9] was used as a guest and encapsulated inside the cages of **1**. Caffeine was loaded into the MOP cages by stirring a solution of **1** and caffeine in DMF at room temperature, followed by EtOAc-assisted recrystallization (see the Supporting Information for details). FTIR spectroscopy, TGA (see Figures S3 and S16), and elemental analysis confirmed the loading of caffeine molecules (ca. 4.85 %) inside the MOP cage. The decrease in surface area of the loaded material, as detected on the basis of the N_2-adsorption isotherm (see Figure S20), suggests that caffeine molecules are encapsulated inside the core of the MOP, and not simply absorbed on the surface. The observed release profile also rules out the possibility of the surface absorption of caffeine molecules, in which case the payload would be expected to come out in a single shot at the very beginning, which would have led to a burst release. Since the observed pattern is one of gradual release, this result confirms the loading as loading inside the pores. When the loaded material was placed in water, the induced interconversion event of the MOP cages resulted in a gradual release of the encapsulated drug over time (Figure 4), as monitored by UV/Vis spectroscopy.

In conclusion, we have synthesized a new soluble copper-based MOP from 5-(prop-2-ynyloxy)isophthalic acid and $Cu(NO_3)_2 \cdot 3H_2O$ which unfolds upon treatment with water. This MOP is highly soluble in DMF, DEF, and DMSO and can be recrystallized readily from these solvents. We have used this MOP as a cage for the encapsulation of active molecules (caffeine), and we have successfully explained the release of the encapsulated guests through an unprecedented hydrolytic MOP-to-MOF conversion. Potential applications in the controlled release of trapped active guest molecules are envisioned for such materials and morphological transitions. We are currently pursuing studies towards the fine-tuning of this phenomenon for the controlled release of encapsulated molecules.

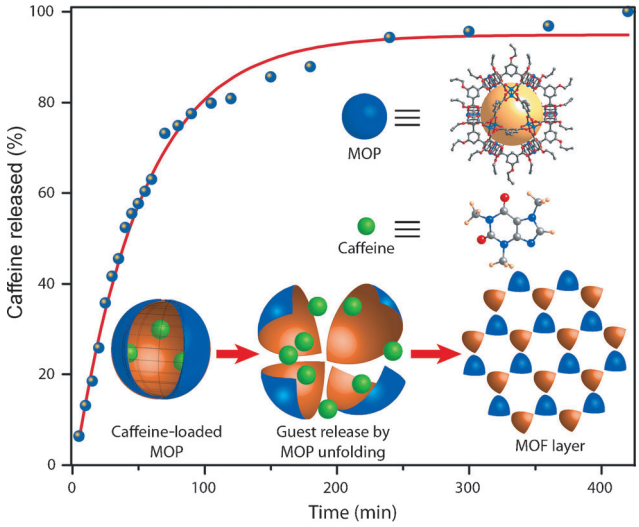

Figure 4. Profile for the release of encapsulated caffeine molecules from the MOP core. A schematic representation of the release driven by the unfolding event is also shown.

Experimental Section

Synthesis of **1**: 5PIA (44 mg, 0.2 mmol) and $Cu(NO_3)_2 \cdot 3H_2O$ (24.2 mg, 0.1 mmol) were dissolved in DMF/EtOH (2:1, v/v; 6 mL), and the resulting mixture was heated at 90 °C for 35 h. Alternatively, the starting materials were dissolved in a mixture of DMF (4 mL) and EtOAc (2 mL), and the resulting mixture was kept at room temperature for 30 h. The polyhedral crystals thus obtained were characterized immediately after removal from the mother liquid (yield of the isolated product: 75 %). FTIR (ATR): $\tilde{\nu}$ =3279 (w), 2119 (w), 1628 cm^{-1} (s); C,H analysis: calcd (%): C 46.13, H 2.61; found: C 46.37, H 2.88.

Synthesis of **3**: Compound **1** or **2** (25 mg, 0.003 mmol) was placed in a 15 mL vial, water (5 mL) was added, and the resulting mixture was heated at 120 °C for 1 h. The hexagonal crystals that formed were filtered and washed with 99.99 % absolute ethanol (yield of the isolated product: 92 %). The crystals were characterized after drying at room temperature. FTIR (ATR): $\tilde{\nu}$ =3287 (w), 2117 (w), 1618 cm^{-1} (s); C,H analysis: calcd (%): C 44.06, H 2.69; found: C 44.09, H 2.77.

Received: August 26, 2013
Published online: November 7, 2013

Keywords: cage compounds · crystal engineering · hydrophobic effect · metal–organic frameworks · self-assembly

[1] a) J. Tranchemontagne, Z. Ni, M. O'Keeffe, O. M. Yaghi, *Angew. Chem.* **2008**, *120*, 5214–5225; *Angew. Chem. Int. Ed.* **2008**, *47*, 5136–5147; b) P. Mal, B. Breiner, K. Rissanen, J. R. Nitschke, *Science* **2009**, *324*, 1697–1699; c) J. R. Li, H. C. Zhou, *Angew. Chem.* **2009**, *121*, 8617–8620; *Angew. Chem. Int. Ed.* **2009**, *48*, 8465–8468; d) M. Jaya Prakash, M. Oh, X. Liu, K. N. Han, G. H. Seong, M. S. Lah, *Chem. Commun.* **2010**, *46*, 2049–2051; e) Q. F. Sun, J. Iwasa, D. Ogawa, Y. Ishido, S. Sato, T. Ozeki, Y. Sei, K. Yamaguchi, M. Fujita, *Science* **2010**, *328*, 1144–1147; f) W. Meng, B. Breiner, K. Rissanen, J. D. Thoburn, J. K. Clegg, J. R. Nitschke, *Angew. Chem.* **2011**, *123*, 3541–3545; *Angew. Chem. Int. Ed.* **2011**, *50*, 3479–3483; g) J. Bunzen, J. Iwasa, P. Bonakdarzadeh, E. Numata, K. Rissanen, S. Sato, M. Fujita, *Angew. Chem.* **2012**, *124*, 3215–3217; *Angew. Chem. Int. Ed.* **2012**, *51*, 3161–3163; h) S. Zarra, M. M. J. Smulders, Q. Lefebvre, J. K. Clegg, J. R. Nitschke,

Angew. Chem. **2012**, *124*, 6988 – 6991; *Angew. Chem. Int. Ed.* **2012**, *51*, 6882 – 6885.

[2] a) B. Moulton, J. Lu, A. Mondal, M. J. Zaworotko, *Chem. Commun.* **2001**, 863 – 864; b) J. Park, S. Hong, D. Moon, M. Park, K. Lee, S. Kang, Y. Zou, R. P. John, G. H. Kim, M. S. Lah, *Inorg. Chem.* **2007**, *46*, 10208 – 10213.

[3] a) H. Furukawa, J. Kim, N. W. Ockwig, M. O'Keeffe, O. M. Yaghi, *J. Am. Chem. Soc.* **2008**, *130*, 11650 – 11661; b) K. Nakabayashi, Y. Ozaki, M. Kawano, M. Fujita, *Angew. Chem.* **2008**, *120*, 2076 – 2078; *Angew. Chem. Int. Ed.* **2008**, *47*, 2046 – 2048; c) M. Jung, H. Kim, K. Baek, K. Kim, *Angew. Chem.* **2008**, *120*, 5839 – 5841; *Angew. Chem. Int. Ed.* **2008**, *47*, 5755 – 5757; d) T. Murase, K. Otsuka, M. Fujita, *J. Am. Chem. Soc.* **2010**, *132*, 7864 – 7865; e) J. R. Li, A. A. Yakovenko, W. Lu, D. J. Timmons, W. Zhuang, D. Yuan, H. C. Zhou, *J. Am. Chem. Soc.* **2010**, *132*, 17599 – 17610; f) S. Horiuchi, T. Murase, M. Fujita, *J. Am. Chem. Soc.* **2011**, *133*, 12445 – 12447; g) Y. Inokuma, M. Kawano, M. Fujita, *Nat. Chem.* **2011**, *3*, 349 – 358; h) I. A. Riddell, M. M. J. Smulders, J. K. Clegg, J. R. Nitschke, *Chem. Commun.* **2011**, *47*, 457 – 459; i) M. M. J. Smulders, J. R. Nitschke, *Chem. Sci.* **2012**, *3*, 785 – 788.

[4] a) S. Horiuchi, Y. Nishioka, T. Murase, M. Fujita, *Chem. Commun.* **2010**, *46*, 3460 – 3462; b) T. Murase, H. Takezawa, M. Fujita, *Chem. Commun.* **2011**, *47*, 10960 – 10962; c) S. Horiuchi, T. Murase, M. Fujita, *Chem. Asian J.* **2011**, *6*, 1839 – 1847; d) J. S. Mugridge, A. Zahl, R. V. Eldik, R. G. Bergman, K. N. Raymond, *J. Am. Chem. Soc.* **2013**, *135*, 4299 – 4306; e) C. J. Hastings, M. P. Backlund, R. G. Bergman, K. N. Raymond, *Angew. Chem.* **2011**, *123*, 10758 – 10761; *Angew. Chem. Int. Ed.* **2011**, *50*, 10570 – 10573; f) Y. Liu, C. Hu, A. Comotti, M. D. Ward, *Science* **2011**, *333*, 436 – 440; g) J. K. Clegg, F. Li, K. A. Jolliffe, G. V. Meehan, L. F. Lindoy, *Chem. Commun.* **2011**, *47*, 6042 – 6044; h) C. R. K. Glasson, J. K. Clegg, J. C. McMurtrie, G. V. Meehan, L. F. Lindoy, C. A. Motti, B. Moubaraki, K. S. Murray, J. D. Cashion, *Chem. Sci.* **2011**, *2*, 540 – 543.

[5] a) S. Zarra, J. K. Clegg, J. R. Nitschke, *Angew. Chem.* **2013**, *125*, 4937 – 4940; *Angew. Chem. Int. Ed.* **2013**, *52*, 4837 – 4840; b) J. R. Li, H. C. Zhou, *Nat. Chem.* **2010**, *2*, 893 – 898; c) S. Sato, Y. Ishido, M. Fujita, *J. Am. Chem. Soc.* **2009**, *131*, 6064 – 6065; d) W. Lu, D. Yuan, A. Yakovenko, H.-C. Zhou, *Chem. Commun.* **2011**, *47*, 4968 – 4970.

[6] D. Zhao, S. Tan, D. Yuan, W. Lu, Y. H. Rezenom, H. Jiang, L.-Q. Wang, H. C. Zhou, *Adv. Mater.* **2011**, *23*, 90 – 93.

[7] a) L. B. Sun, J. R. Li, W. Lu, Z. Y. Gu, Z. Luo, H. C. Zhou, *J. Am. Chem. Soc.* **2012**, *134*, 15923 – 15928; b) T. F. Liu, Y. P. Chen, A. A. Yakovenko, H. C. Zhou, *J. Am. Chem. Soc.* **2012**, *134*, 17358 – 17361.

[8] M. Eddaoudi, J. Kim, J. B. Wachter, H. K. Chae, M. O'Keeffe, O. M. Yaghi, *J. Am. Chem. Soc.* **2001**, *123*, 4368 – 4369.

[9] a) P. Horcajada, T. Chalati, C. Serre, B. Gillet, C. Sebrie, T. Baati, J. F. Eubank, D. Heurtaux, P. Clayette, C. Kreuz, J.-S. Chang, Y. K. Hwang, V. Marsaud, P.-N. Bories, L. Cynober, S. Gil, G. Férey, P. Couvreur, R. Gref, *Nat. Mater.* **2010**, *9*, 172 – 178; b) D. Cunha, M. B. Yahia, S. Hall, S. R. Miller, H. Chevreau, E. Elkaïm, G. Maurin, P. Horcajada, C. Serre, *Chem. Mater.* **2013**, *25*, 2767 – 2776; c) N. Liédana, A. Galve, C. Rubio, C. Tellez, J. Coronas, *ACS Appl. Mater. Interfaces* **2012**, *4*, 5016 – 5021.